

# Laser Ablation of a YBCO Target at 266 nm and 1064 nm: Reactive Scattering of a YBCO Plume and an Oxygen Jet

Ji Youn Moon and Seung Min Park\*

Department of Chemistry, Kyunghee University, Seoul 130-701, Korea

Received June 21, 1999

Pulsed laser ablation of solid targets has been a research topic of utmost interest due to its wide applications in the growth of thin films of ceramic superconductors, metals, and refractory materials.<sup>1</sup> Laser ablation is attractive as a tool for deposition of thin films since a stoichiometric transfer of multielement target material to a substrate is possible and the deposition may be performed at a relatively low temperature.<sup>1</sup>

For some target materials like oxides or nitrides, however, the stoichiometries of the films deposited by pulsed laser deposition often do not represent those of the bulk, which leads to a serious deficiency of oxygen or nitrogen.<sup>2</sup> Recently, use of synchronized pulsed jet of reactive gas has been suggested to supply deficient chemical species to the plume and to reduce the background pressure below  $10^{-3}$  Torr.<sup>3</sup> This pressure is low enough for reflection high energy electron diffraction (RHEED), making possible *in situ* analysis and control of the film deposition.

In pulsed laser deposition of thin films, one of the most important parameters is the laser wavelength, which plays mainly in the effectiveness of the absorption of the laser power into the target.<sup>1</sup> The absorption coefficient  $\alpha$  determines the penetration depth. The size and density of particulates which affect the quality of thin films and the target topography are strongly dependent on the penetration depth. For oxide superconductors like YBCO ( $\text{YBa}_2\text{Cu}_3\text{O}_{7-x}$ ), the penetration depth is known to be larger in the near IR than in the UV. Therefore, UV wavelengths are preferred in the deposition of oxide superconductors by laser ablation.

Also, the effects of laser wavelength on the so-called "plume chemistry" have to be considered in pulsed laser deposition of thin films especially when reactive scatterings and photochemical phenomena are expected by injection of reactive gas to the plume (laser-induced plasma, plasma produced by irradiation of solid surfaces). That is, formation and dissociation of oxide molecules or ions in a plume would be highly dependent on the laser wavelength chosen for laser ablation of a solid target. For multielement targets like YBCO, there is no doubt that densities of different oxides and their relative enrichment in the plume would affect the film growth and its quality significantly.

Here, we report a time-of-flight (TOF) studies of ions produced via laser ablation of a YBCO target with and without oxygen jet. The pulsed oxygen source is employed to investigate the reactive scatterings in the plume.<sup>4</sup> Two different wavelengths (266 nm and 1064 nm), one in UV and the other in IR region, are selected to examine the effects of

laser wavelength on the TOF spectra of ions produced by laser ablation. Formation mechanisms of diatomic oxide ions and characteristics of the plume are investigated by analysis of TOF spectra.

## Experimental Section

The laser ablation apparatus is depicted in Figure 1. It consists of a target chamber and an analysis chamber, which are differentially pumped and separated by a skimmer (R. M. Jordan Co.) with an orifice diameter of 0.97 mm. Laser ablation and subsequent reactions occur in the target chamber, where a 25.4 mm diameter  $\text{YBa}_2\text{Cu}_3\text{O}_{7-x}$  target (Superconductive Components, Inc., 99.99%) is mounted and rotated by a standard rotary motion feedthrough (MDC K150-BRM-01) to avoid a target aging effect. The distance from the target to the orifice of the skimmer is 1.7 cm. 266 nm or 1064 nm radiation from an Nd:YAG laser (Spectra-Physics GCR150-10) is focused onto the target by using a 300 mm lens at an incident angle of  $50^\circ$ .

A pulsed valve (General Valve Series 9), synchronized with the laser pulse, is also mounted inside the target chamber to blow an oxygen jet to the plume so that the propagation axis of the jet is perpendicular to the direction of plume expansion as illustrated in Figure 1. Typical equilibrium pressures of the target and the analysis chamber with the laser impinging the target and the oxygen jet of 250  $\mu\text{s}$  duration on are  $4 \times 10^{-6}$  Torr and  $2 \times 10^{-7}$  Torr, respectively.

The analysis chamber is equipped with a quadrupole mass spectrometer (VG SX300). Ion optics in front of the quadrupole housing are grounded and the ionizer is turned off during the experiment to detect ions only. The flight distance of ions, 20.4 cm, is defined as the length between the target and

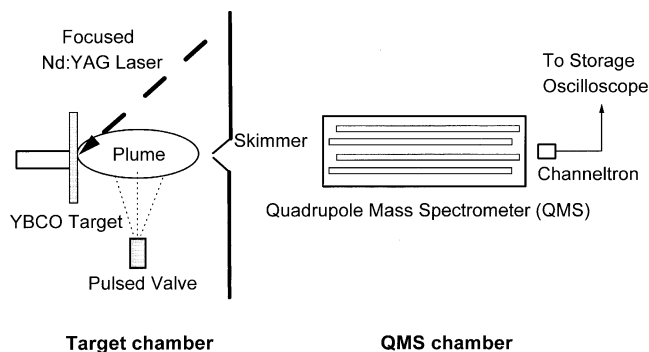
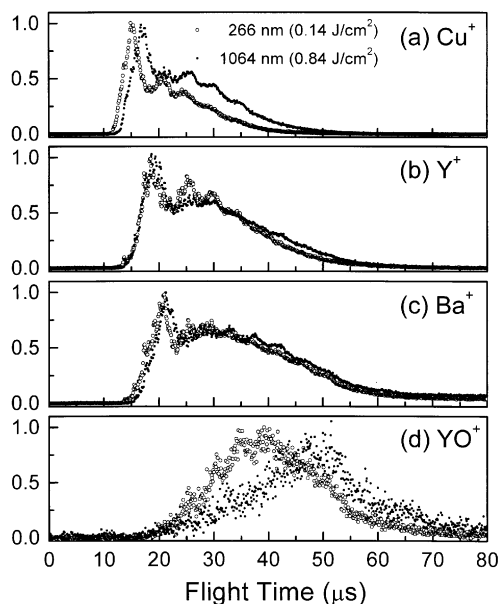


Figure 1. The schematic diagram of the experiment.



**Figure 2.** Normalized time-of-flight spectra of (a)  $\text{Cu}^+$ , (b)  $\text{Y}^+$ , (c)  $\text{Ba}^+$ , and (d)  $\text{YO}^+$  ions obtained at 266 nm ( $0.14 \text{ J/cm}^2$ , open circles) and 1064 nm ( $0.84 \text{ J/cm}^2$ , filled circles) with the oxygen jet off.

an entrance hole to a detector. One hundred laser shots are irradiated on the rotating target surface, each giving a TOF spectrum. These spectra are averaged into a single TOF spectrum by a storage oscilloscope (LeCroy 9361, 300 MHz).

### Results and Discussion

Figure 2 shows normalized TOF spectra of  $\text{Cu}^+$ ,  $\text{Y}^+$ ,  $\text{Ba}^+$ , and  $\text{YO}^+$  ions obtained at 266 nm ( $0.14 \text{ J/cm}^2$ ) and 1064 nm ( $0.84 \text{ J/cm}^2$ ) with the oxygen jet off. The laser fluences are chosen such that the TOF distributions and signal magnitudes of  $\text{Ba}^+$  ions at the two wavelengths are similar with each other. The TOF spectrum of each ion is measured at the mass of the most abundant isotope. TOF spectra of  $\text{CuO}^+$  and  $\text{BaO}^+$  ions are not obtainable presumably because the relative enrichment of oxide ions in the plume depends on the plume temperature and dissociation energies of oxide ions ( $D_0(\text{CuO}) = 1.6 \text{ eV}$ ,<sup>5</sup>  $D_0(\text{YO}) = 7.2 \text{ eV}$ ,<sup>6</sup> and  $D_0(\text{BaO}) = 4.1 \text{ eV}$ <sup>7</sup>). The TOF spectra of  $\text{YO}^+$  and  $\text{BaO}^+$  ions with the oxygen jet on and off at the two wavelengths are shown in Figure 3. Even with the oxygen jet on,  $\text{CuO}^+$  ions are not observed due to the shallow well depth of the potential energy curve of  $\text{CuO}^+$ . The amounts of  $\text{YO}^+$  and  $\text{BaO}^+$  ions in the plume, however, show a fair and a dramatic increase, respectively, as oxygen molecules are supplied to the plume.

The TOF spectra of metal ions display single broad distributions near the threshold fluences of each ion. At low laser fluences near the threshold of ion ejection, ions are produced by direct ejection and ionization of neutral atoms in the plume.<sup>8</sup> Metal ions produced as results of dissociation and/or ionization of metal oxides and their ions are also expected to

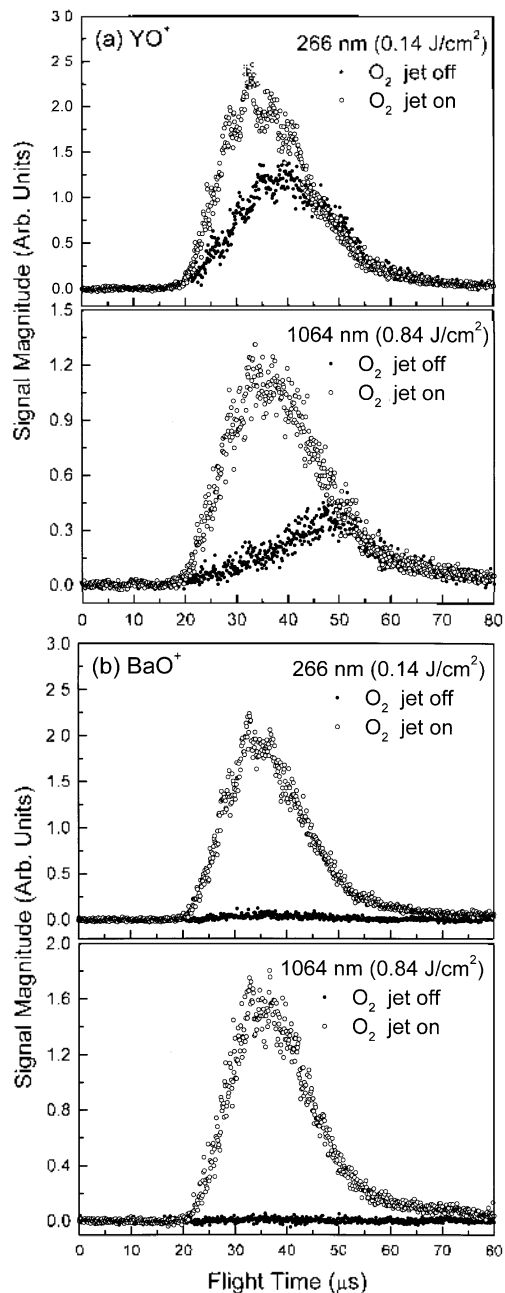


**Figure 3.** Time-of-flight spectra of (a)  $\text{YO}^+$  and (b)  $\text{BaO}^+$  with the oxygen jet off and on (duration = 250  $\mu\text{s}$ ) at 266 nm ( $0.14 \text{ J/cm}^2$ , open circles) and 1064 nm ( $0.84 \text{ J/cm}^2$ , filled circles).

be included in this broad distribution. As the laser fluence is increased, a high-energy peak smears out as a shoulder on the low-energy peak as shown in Figure 2(a)-2(c). Similar peak splitting has been reported in the laser ablation of ZnO by Leuchtner,<sup>8</sup> who proposed the possibility of formation of doubly charged metal ions and their recombination with electrons giving high-energy peak in the TOF spectra of  $\text{Zn}^+$  ions at high laser fluences.

For MO<sup>+</sup> ions (MO<sup>+</sup> = YO<sup>+</sup> or BaO<sup>+</sup>), such prominent high-energy component is not observed. The TOF spectra of MO<sup>+</sup> ions exhibit single broad distributions over the laser fluence range of our experiment ( $0.045 \text{ J/cm}^2$ - $0.14 \text{ J/cm}^2$  and

**Table 1.** Mean kinetic energies of ions (eV)

wavelength	O <sub>2</sub> jet	O <sup>+</sup>	Cu <sup>+</sup>	Y <sup>-</sup>	YO <sup>+</sup>	Ba <sup>-</sup>	BaO <sup>-</sup>
266 nm (0.14 J/cm <sup>2</sup> )	off	13.2	37.6	30.2	15.9	34.7	-
	on	13.2	36.6	30.3	18.9	33.3	26.1
1064 nm (0.84 J/cm <sup>2</sup> )	off	16.3	27.5	28.3	11.8	29.8	-
	on	17.0	26.5	27.3	16.9	27.9	24.0

0.40 J/cm<sup>2</sup>-0.93 J/cm<sup>2</sup> at 266 nm and 1064 nm, respectively). The TOF spectra of YO<sup>+</sup> at 266 nm and 1064 nm with the oxygen jet off (Figure 2(d)) are quite different with each other while those with the oxygen jet on (Figure 3(a)) look almost alike. Without the oxygen jet, YO<sup>+</sup> ions are mostly produced by collisional ionization of slow YO molecules at 1064 nm although the possibility of direct ablation of YO<sup>+</sup> can not be completely ruled out. At 266 nm, photoionization of YO molecules in the early stage of plume formation is also expected to contribute to the formation of the faster YO<sup>+</sup> ions. Therefore, TOF distribution of YO<sup>+</sup> ions at 266 nm is shifted relatively to the left as shown in Figure 2(d). With the oxygen jet on, density of MO<sup>+</sup> ions in the plume is substantially increased by the M<sup>+</sup> + O<sub>2</sub> reaction<sup>5,6</sup> at both wavelengths. MO<sup>+</sup> ions thus produced have higher kinetic energies as shown in Table 1 and result in similar TOF distributions at the two wavelengths when the oxygen jet is on.

The most striking differences between the TOF spectra at 266 and 1064 nm are found for O<sup>+</sup> as shown in Figure 4. The TOF spectra of O<sup>+</sup> ions display very clear bimodal distributions. The fast peak is considered to correspond to the O<sup>+</sup> ions produced by direct ejection<sup>9</sup> while the slow peak originates from neutral O atoms ionized in the plume. O atoms are enriched in the plume by dissociation of metal oxides as well as direct ejection from the target surface. With the oxygen jet on, it is found that the peak magnitude of the slow component diminishes remarkably while that of the fast one remains almost unchanged. Since the neutral O atoms which are the origin of the slow peak have small kinetic energies, they are easily swept away via elastic or inelastic scatterings

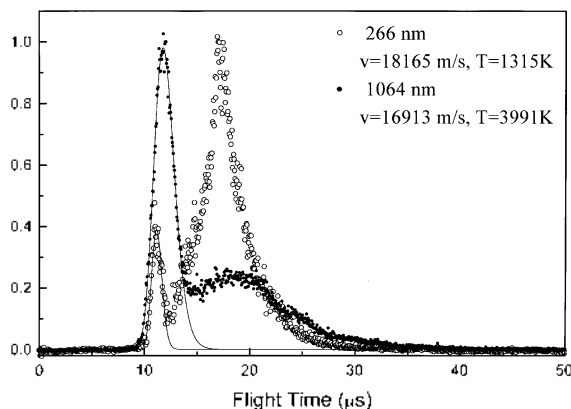


**Figure 4.** Normalized time-of-flight spectra of O<sup>+</sup> ions with the oxygen jet off at 266 nm (0.14 J/cm<sup>2</sup>, open circles) and 1064 nm (0.84 J/cm<sup>2</sup>, filled circles). The solid lines are shifted Maxwell-Boltzmann fits with a stream velocity and temperature as fitting parameters.

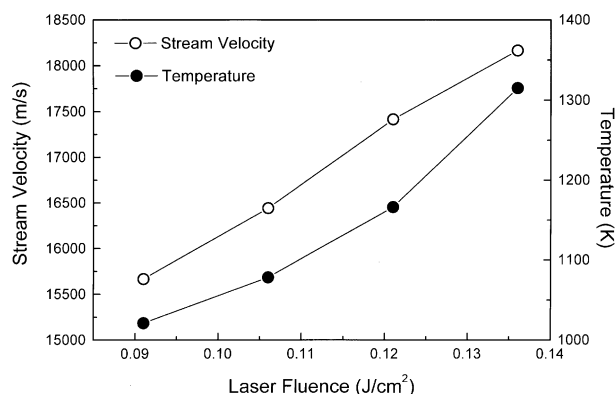


**Figure 5.** The stream velocity (open circles) and temperature (filled circles) of O<sup>+</sup> ions (fast component) at 266 nm obtained by shifted Maxwell-Boltzmann fits as a function of laser fluence. The pulsed jet is off.

with oxygen molecules. Recombination of O atoms giving neutral oxygen molecules with a supply of oxygen molecules to the plume is also expected.<sup>10</sup>

Dissociation of oxides followed by ionization of neutral O atoms is more efficient at 266 nm than at 1064 nm, making the plume enriched with relatively slow O<sup>+</sup> ions. Direct ejection of O<sup>+</sup> turns out to be more efficient at higher fluence of 1064 nm than at lower fluence of 266 nm, the reason of which is not clear yet. As long as the bimodal distribution is clear and the direct ejection mechanism is assigned to the high-energy peak of the O<sup>+</sup> TOF spectra excluding any other mechanisms which would cause certain broadening of TOF distribution, a shifted Maxwell-Boltzmann fitting<sup>11</sup> can be attempted to fit the early part of the spectra. Since the TOF distributions of O<sup>+</sup> ions are well fit by shifted Maxwell-Boltzmann distributions, it may be assumed that the directly-ejected O<sup>+</sup> ions reach thermal equilibrium as they expand.

The temperature of O<sup>+</sup> ions produced by laser ablation at 1064 nm is significantly higher than at 266 nm, which would originate not only from the total amount energy deposited but also from the efficient heating of plasma by inverse Bremsstrahlung absorption at 1064 nm.<sup>1</sup> Figure 5 shows the dependence of the stream velocity and temperature on the laser fluence. The increase of stream velocity with laser fluence can be explained by the space charge effect.<sup>4</sup> The fact that the temperature of ions directly ejected via a nonthermal process increases with increasing laser fluence indicates that the photon energy is absorbed by the plume.

### Summary

Formation mechanisms of metal oxide ions in a reactive atmosphere have been studied by a crossed beam scattering of a plume produced by laser ablation of a YBa<sub>2</sub>Cu<sub>3</sub>O<sub>7-x</sub> target and an oxygen jet. Monovalent metal ions are produced by direct ejection, ionization of neutral atoms, and recombination of doubly charged ions with electrons. Metal oxide ions are mostly produced by ionization of neutral oxide molecules without ambient oxygen molecules. With the oxygen jet on, reaction of metal ions with oxygen molecules contrib-

utes significantly to the enrichment of metal oxide ions. Relative population of each metal oxide ion in the plume is determined by bond dissociation energies of MO and MO<sup>+</sup>, ionization potential of MO, and reaction cross section of the M<sup>+</sup> + O<sub>2</sub> → MO<sup>+</sup> + O reaction when oxygen molecules are supplied to the plume. Therefore, it would be necessary to choose an appropriate wavelength and its fluence to achieve an optimal condition for the growth of YBCO thin film by using pulsed laser deposition.

**Acknowledgment.** SMP is grateful to Research Institute for Basic Sciences, Kyunghee University (University Research Fund, 1998).

### References

1. *Pulsed Laser Deposition of Thin Films*: Chrisey, D. B.; Hubler, G. K. Ed.; Wiley-Interscience: New York, U. S. A., 1994.
  2. Chae, H.; Park, S. M. *Appl. Surf. Sci.* **1998**, *127-129*, 304.
  3. Willmott, P. R.; Timm, R.; Huber, J. R. *J. Appl. Phys.* **1997**, *83*, 2082.
  4. Park, S. M.; Moon, J. Y. *J. Chem. Phys.* **1998**, *109*, 8124.
  5. Fisher, E. R.; Elkind, J. L.; Clemmer, D. E.; Georgiadis, R.; Loh, S. K.; Aristov, N.; Sunderlin, L. S.; Armentrout, P. B. *J. Chem. Phys.* **1990**, *93*, 2676.
  6. Sievers, M. R.; Chen, Y.-M.; Armentrout, P. B. *J. Chem. Phys.* **1996**, *105*, 6322.
  7. Huber, K. P.; Herzberg, G. *Molecular Spectra and Molecular Structure. IV. Constants of Diatomic Molecules*. Van Nostrand Reinhold: New York, U. S. A., 1979.
  8. Leuchtner, R. E. *Appl. Surf. Sci.* **1998**, *127-129*, 626.
  9. Knot, M. L.; Feibelman, P. J. *Phys. Rev. Lett.* **1978**, *40*, 964.
  10. Park, S. M.; Chae, H.; Wee, S.; Lee, I. *J. Chem. Phys.* **1998**, *109*, 928.
  11. Zheng, J. P.; Huang, Z. Q.; Shaw, D. T.; Kwok, H. S. *Appl. Phys. Lett.* **1989**, *54*, 280.
-